Behaviour of chromium isotopes in the eastern sub-tropical Atlantic Oxygen Minimum Zone

Heather J. Goring-Harford1*, J. K. Klar1,2, Christopher R. Pearce3, Douglas P. Connelly3, Eric P. Achterberg4, Rachael H. James1

1 Ocean and Earth Science, National Oceanography Centre, University of Southampton Waterfront Campus, Southampton, SO14 3ZH, UK.

2LEGOS, Université de Toulouse, CNES, CNRS, IRD, UPS, 14 Avenue Edouard Belin, 31400 Toulouse, France

3 Marine Geoscience, National Oceanography Centre, University of Southampton Waterfront Campus, Southampton, SO14 3HZ, UK.

4 GEOMAR Helmholtz Centre for Ocean Research, Kiel, Germany

*Corresponding Author

Email address: h.j.goring-harford@soton.ac.uk

Phone number: +442380596666

Abstract

Constraints on the variability of chromium (Cr) isotopic compositions in the modern ocean are required to validate the use of Cr isotopic signatures in ancient authigenic marine sediments for reconstructing past levels of atmospheric and ocean oxygenation. This study presents dissolved Cr concentrations (CrT, where CrT = Cr(VI) + Cr(III)) and Cr isotope data (δ^{53}Cr) for shelf, slope and open ocean waters within the oxygen minimum zone (OMZ) of the eastern sub-tropical Atlantic Ocean. Although dissolved oxygen concentrations were as low as 44-90 μmol kg-1 in the core of the OMZ, there was no evidence for removal of Cr(VI). Nonetheless, there was significant variability in seawater δ^{53}Cr, with values ranging from 1.08 to 1.72‰. Shelf CrT concentrations were slightly lower (2.21 ± 0.07 nmol kg-1) than in open ocean waters at the same water depth (between 0 and 160m, 2.48 ± 0.07 nmol kg-1). The shelf waters also had higher δ^{53}Cr values (1.41 ± 0.14‰ compared to 1.18 ± 0.05‰ for open ocean waters shallower than 160m). This is consistent with partial reduction of Cr(VI) to Cr(III), with subsequent removal of isotopically light Cr(III) onto biogenic particles. We also provide evidence for input of relatively isotopically heavy Cr from sediments on the shelf. Intermediate and deep water masses (AAIW and NADW) show a rather limited range of δ^{53}Cr values (1.19 ± 0.09‰) and inputs of Cr from remineralisation of organic material or re-oxidation of Cr(III) appear to be minimal. Authigenic marine precipitates deposited in deep water in the open ocean therefore have the potential to faithfully record seawater δ^{53}Cr, whereas archives of seawater δ^{53}Cr derived from shelf sediments must be interpreted with caution.

1. Introduction

Analyses of the chromium (Cr) isotopic composition of authigenic marine sediments are being used to reconstruct the Cr isotopic composition of ancient seawater and, in turn, to provide constraints on the evolution of atmospheric oxygen and the redox history of the oceans (Crowe at al., 2013; Frei et al., 2009; Planavsky et al., 2014). This is because Cr has two stable valence states at Earth surface conditions, Cr(III) and Cr(VI), and mass dependent fractionation of the four stable Cr isotopes (50Cr, 52Cr, 53Cr and 54Cr) occurs during oxidation and reduction reactions (Ellis et al., 2002; Schauble et al., 2004; Zink et al., 2010; Døssing et al., 2011; Kitchen et al., 2012). Moreover, these valence states have different solubilities; Cr(VI) is relatively soluble whereas Cr(III) is not. Chromium isotope ratios are expressed in delta notation relative to the international reference material NBS979 as follows (equation 1):

$$\delta^{53}Cr\ (‰) = \left[\frac{\left(^{53}Cr/^{52}Cr\right)_{sample}}{\left(^{53}Cr/^{52}Cr\right)_{NBS979}} - 1 \right] \times 1000 \tag{1}$$

Application of the Cr isotope proxy requires a detailed process-based understanding of the behaviour of Cr and its isotopes in the modern ocean.

1.1 Distribution of Cr in seawater

Chromium (Cr) is a trace element in seawater and, although it has a relatively long residence time of ~9500 years (Reinhard et al., 2013), its concentration is variable and usually within the range 0.9 to 6.5 nM (Campbell and Yeats 1981; Cranston 1983; Jeandel and Minster 1984; Achterberg and Berg 1997; Sirinawin et al. 2000; Connelly et al. 2006; Bonnand et al. 2013; Scheiderich et al. 2015). In oxygenated seawater, Cr is present primarily as Cr(VI) in the chromate oxyanion, CrO_4^{2-} and, to a lesser extent as Cr(III) in aquahydroxyl or hydroxyl ions (Elderfield, 1970). Chromium changes valence state from Cr(VI) to Cr(III) under mildly reducing conditions and, while Cr(VI) is not significantly particle reactive and is only weakly held on most mineral surfaces (Zachara et al., 1988; Gaillardet et al., 2003), Cr(III) species readily adsorb to biogenic particles (Semeniuk et al., 2016), authigenic precipitates (Crawford et al., 1993) and sediments (Schroeder and Lee, 1975; Richard and Bourg, 1991).

During periods of high biological productivity, Cr(III) can constitute up to ~50% of the dissolved Cr inventory in the upper water column (Achterberg and Berg, 1997; Connelly et al., 2006). Chromium is not thought to be a nutrient for marine bacteria and phytoplankton,

but inadvertent biological uptake is well documented (Wang and Dei, 2001; Sikora et al., 2008; Li et al., 2009; Basu et al., 2014) and may be responsible for reduction of Cr(VI) in surface waters. High concentrations of Fe(II) and organic material in surface waters can also facilitate reduction of Cr(VI) (Døssing et al., 2011; Kitchen et al., 2012). Organic molecules can reduce Cr(VI) in their own right or support reduction by other mechanisms (Jamieson-Hanes et al., 2012; Kitchen et al., 2012), and they can also act to solubilise Cr(III) (Kaczynski and Kieber, 1994).

Reduction of Cr(VI) may also occur in those parts of the ocean that have relatively low concentrations of dissolved oxygen. Low-oxygen waters (<5 μmol kg-1 of dissolved O2) from within the 'oxygen minimum zone' (OMZ) in the tropical East Pacific were found to be depleted in Cr(VI) relative to adjacent oxygenated waters, and concentrations of dissolved Cr(III) and particulate Cr were highest at the top of the OMZ (Murray et al., 1983; Rue et al., 1997). In the Saanich Inlet, an intermittently anoxic fjord, Cr(III) concentrations were close to zero in the upper oxygenated waters whereas Cr(III) constituted >70% of total dissolved Cr in deep anoxic waters (Emerson et al., 1979).

Reduction of Cr(VI) in surface waters and uptake of Cr(III) on particles means that total dissolved Cr concentrations (CrT, where CrT = Cr(VI) + Cr(III)) in the surface ocean are typically slightly lower than they are at depth (Campbell and Yeats, 1981; Cranston, 1983; Dauby et al., 1994; Achterberg and Berg, 1997; Connelly et al., 2006). However, in some parts of the ocean, concentrations of CrT in surface waters may be relatively high due to atmospheric inputs (Achterberg and Berg, 1997), and inputs of Cr from marine sediments and hydrothermal vents can result in relatively high concentrations close to the seabed at some locations (up to 20 nmol kg-1; Jeandel and Minster 1984; Sander and Koschinsky 2000). If there are no external inputs of Cr and rates of biological activity are low, then CrT concentrations may simply reflect those of newly formed water masses that are subducted into the interior ocean (Sirinawin et al., 2000), or mixing between different water masses (Scheiderich et al., 2015).

1.2 Cr isotope composition of seawater

To date there are only a handful of studies of the isotopic composition of CrT in seawater, and δ53Cr values reported for seawater range between 0.13 and 1.55‰ (Bonnand et al. 2013; Paulukat et al. 2015; Pereira et al. 2015; Scheiderich et al. 2015; Economou-Eliopoulos et al. 2016; Holmden et al. 2016; Paulukat et al. 2016). Most of these seawater samples have δ53Cr

values that are higher than those for crustal rocks (-0.12 ± 0.10‰; Schoenberg et al. 2008). As rivers are the main source of Cr to the oceans (90-98%; Chester and Murphy 1990; Bonnand et al. 2013; McClain and Maher 2016), this suggests either that (i) isotopically heavy Cr is preferentially released during weathering processes, (ii) the weathering signal is modified during transport to the oceans (e.g. during estuarine mixing), or (iii) Cr isotopes are fractionated by Cr cycling within the oceans.

There is a growing body of evidence that indicates that oxidative weathering preferentially retains light Cr isotopes in the solid phase (Frei et al., 2009; Crowe et al., 2013; Frei and Polat, 2013; Berger and Frei, 2014; Frei et al., 2014; Planavsky et al., 2014; D'Arcy et al., 2016). Water samples from fully oxic groundwater recharge regions are reported to have $\delta53Cr$ values of 1.2 – 2.3‰ (Izbicki et al., 2008), and most river waters that drain into the sea that have been analysed to date are enriched in heavy Cr isotopes ($\delta53Cr = 0.43 \pm 0.38$‰ 1SD, n = 46; D'Arcy et al. 2016, Frei et al. 2014, Paulukat et al. 2015, Wu et al. 2017) relative to crustal rocks. On the other hand, paleosols weathered under oxic conditions (Crowe et al., 2013; Frei and Polat, 2013) and modern soils are enriched in light Cr isotopes (modern soil $\delta53Cr = -0.21 \pm 0.11$‰ 1SD, n = 74; Frei et al. 2014; D'Arcy et al. 2016; Wu et al. 2017). The exact mechanisms that lead to fractionation of Cr isotopes during oxidation reactions are, however, unclear, and laboratory experiments indicate that under some circumstances, oxidation of Cr(III) to Cr(VI) could alternatively lead to retention of heavy Cr isotopes in the residual solid phase (Bain and Bullen, 2005; Zink et al., 2010; Joshi et al., 2011).

The isotopic signal of Cr derived from weathering processes is potentially modified during river transport and/or estuarine mixing. Both Cr(III) and Cr(VI) species have been observed in the dissolved phase in rivers (Cranston and Murray, 1980; Dolamore-Frank, 1984; Kieber and Helz, 1992; Abu-Saba and Flegal, 1995; Gardner and Ravenscroft, 1996; Abu-Saba and Flegal, 1997; Saputro et al., 2014; McClain and Maher, 2016) and there is some evidence for reduction of Cr(VI) in rivers and estuaries in the presence of reductants including Fe(II) and organic molecules (Cranston and Murray, 1980; Dolamore-Frank, 1984; Kieber and Helz, 1992; Saputro et al., 2014; D'Arcy et al., 2016). Theoretical studies and laboratory experiments have shown that reduction of Cr(VI) fractionates Cr isotopes, with enrichment of light Cr isotopes (by as much as -10‰ relative to the initial Cr(VI) solution) in the Cr(III) that forms (Schauble et al., 2004; Sikora et al., 2008; Zink et al., 2010; Døssing et al., 2011; Kitchen et al., 2012). Reduction of Cr(VI) to Cr(III) during mixing between freshwater and

seawater was invoked to explain enrichment of heavy Cr isotopes in Southampton Water compared to Atlantic seawater (Bonnand et al., 2013), and reduction by organic molecules was proposed to cause the same effect in the Glenariff River (D'Arcy et al., 2016). As there are in total only 7 published measurements of δ^{53}Cr in estuarine waters to date (Frei et al., 2014; Paulukat et al., 2015; D'Arcy et al., 2016), and corresponding salinity measurements have not been reported, the behaviour of Cr isotopes during estuarine mixing is, as yet, unknown.

Assessment of the effects of internal cycling of Cr within the oceans on the distribution of Cr isotopes is hampered by the overall lack of δ^{53}Cr data for seawater and especially the absence of full depth profiles for most parts of the ocean. Five seawater samples collected between 30 and 2290 m depth from a station in the oligotrophic Argentine Basin in the South Atlantic had δ^{53}Cr values of between 0.412 and 0.664‰ (Bonnand et al., 2013). The δ^{53}Cr value of the sample from 30 m depth was lower (0.412‰) than the δ^{53}Cr values for the rest of the profile (0.491 – 0.664‰) but there was little difference in the Cr concentrations of surface and deep waters (Bonnand et al., 2013). A better resolved vertical profile has been obtained by combining data from three stations (total of 15 samples) in the open Beaufort Sea together with 4 samples collected from the shelf (Scheiderich et al., 2015). Samples from the surface mixed layer (SML) that had relatively low salinity (25.3 – 29.9) had the lowest Cr concentrations (1.2 – 1.5 nmol kg-1) and relatively high δ^{53}Cr values (1.47 to 1.53‰). Seawater samples recovered from below the SML exhibited a negative correlation between lnCrT and δ^{53}Cr. This was suggested to indicate that the Cr isotopic composition of seawater is principally controlled by reduction of Cr(VI) (and subsequent removal of Cr(III)) in surface waters and OMZs (with ΔCr(III)-Cr(VI) = -0.80 ± 0.03‰, where ΔCr(III)-Cr(VI) = δ^{53}CrCr(III) - δ^{53}CrCr(VI)), and input of Cr at depth due to re-oxidation of Cr(III) from sinking particles or seafloor sediments (Scheiderich et al., 2015).

To better assess the controls on the Cr isotopic composition of seawater, we collected vertical profiles of seawater from the continental shelf, slope and open ocean in the eastern equatorial Atlantic Ocean. All of the stations intersect low oxygen (dysoxic - see Table 1 for definition) waters of the eastern Atlantic OMZ. We show that Cr(VI) is unlikely to be reduced under dysoxic conditions, but that CrT and δ^{53}Cr are affected by biological processes and inputs from sediments on the shelf whereas deep waters are relatively unaffected by internal Cr cycling. We also discuss the implications of our results for the interpretation of Cr isotopic values in marine sedimentary archives.

2. Study area

Water samples were collected from the eastern Atlantic OMZ at six stations during RRS Discovery cruise D361 (GEOTRACES transect GA06) between 7 February and 19 March 2011, as part of the GEOTRACES project. Four stations (stations 2-5) were located above the Senegalese shelf and a fifth (station 18) in the North Atlantic Ocean approximately halfway between the Senegalese coast and the mid-Atlantic ridge, all at a latitude of ~12°N. A sixth station (station 11.5) was located in the South Atlantic Ocean at a latitude of 3°S (Figure 1; Table 2).

Senegalese coastal waters are located in the southern extent of the North West African upwelling system. Upwelling only occurs there in the boreal winter and spring when trade winds are strong, and the vertical extent of upwelling is relatively shallow compared to more northerly regions, with the deepest upwelled waters originating from the top of the thermocline (~100m; Pelegrí and Benazzouz 2015). Nonetheless, elevated nutrient levels in the upper 100m of the water column allow enhanced biological activity on the shelf and slope. In addition to coastal upwelling, the Guinea Dome upwelling system is also located in the study area.

Below the coastal upwelling system, South Atlantic Central Water (SACW) is found at depths of ~150-500m. This water mass is transferred to the South Atlantic Ocean from the Indian Ocean via the Aghulas current, and contains components of both Indian Central Water (ICW) and South Pacific Central Water (SPCW; Tomczak and Godfrey 2003). It crosses the Atlantic basin via the Benguela current, and travels north with the North Brazilian Undercurrent. Beyond, in the sub-tropical and equatorial regions, the pathways of SACW are highly complex and seasonally variable (Stramma and England, 1999).

The SACW meets well-ventilated North Atlantic Central Water (NACW) at the Cape Verde Convergence Zone at approximately 20°N (Figure 1). The NACW is consequently deflected towards the west forming the south-eastern corner of the North Atlantic sub-tropical gyre. This means that NACW inputs at 12°N are negligible and subsequent ventilation of SACW is prevented (Stramma et al., 2005). This contributes to the presence of a poorly ventilated 'shadow zone' between the sub-tropical gyre and equatorial current systems, in which our study area lies (Zenk et al., 1991). Dissolved oxygen concentrations on the shelf and slope are also depleted as large quantities of organic matter sink and decay. The combined effects of poor ventilation and high biological productivity in surface waters cause a dysoxic OMZ (44-

90 μmol kg-1 O2) at 200-800m depth, though the waters do not become suboxic (as defined in Table 1) as in OMZs in the Indian and Pacific Oceans (Helly and Levin, 2004). Highly oxygenated Antarctic Intermediate Water (AAIW) bounds the OMZ from below and is identified by a salinity minimum at 600-1000m, whilst NADW occurs between 1000m and the seafloor, though the deepest stations may be influenced by Antarctic Bottom Water (AABW) (Stramma and England, 1999; Stramma et al., 2005).

At 3°S (station 11.5) the water column structure is similar to that at 12°N, with the exception that Upper Circumpolar Deep Water (UCDW) is found between AAIW and NADW at 1000-1300m. SACW at this station is fed by both oxygen poor equatorial waters and oxygen rich waters from the south (Stramma and Schott, 1999). This results in higher average O2 concentrations within the SACW compared to the other stations, though the OMZ is still well defined between 200 and 600m.

3. Methods

3.1 Sample collection

A trace metal clean CTD system equipped with modified Ocean Test Equipment Inc. (OTE) bottles was used to collect water samples of ~3L volume. The OTE bottles were transferred to a class 100 clean container aboard the RRS Discovery and seawater was filtered through pre-rinsed Supor Acropak filters (0.2 μm) or acid cleaned polyethersulfone filters (0.45 μm) into acid washed 1L bottles. Samples were acidified to pH 2 (Romil UpA HCl) and double bagged for storage at room temperature at the National Oceanography Centre, Southampton (Klar et al., this issue). From these samples, aliquots of 1-2 L were taken for Cr isotope analysis and the rest was used for Fe isotope analysis (Klar et al., this issue).

3.2 Analysis of Cr concentration and isotopic values

The total Cr concentration (CrT, where CrT = Cr(VI) + Cr(III)) and Cr isotopic values of seawater samples were determined by multi-collector inductively coupled plasma mass spectrometry (MC-ICP-MS) using a double spike technique based on that described by Bonnand et al. 2013. Processing of the samples was carried out in a class 100 clean laboratory. All acid reagents were sub-boiled while ammonia and H2O2 were Romil UpA and Fluka TraceSELECT grades, respectively.

3.2.1 Preliminary determination of CrT

In order to optimise the ratio of natural Cr to double spike Cr for isotopic measurements, concentrations of CrT were first determined for selected samples using a single spike isotope dilution (ID) technique (Bedson, 2007). The method followed a similar procedure to that described in Section 3.2.2, but used a single ^{53}Cr spike and smaller sample volumes (~200 mL). Seawater CrT concentrations were determined from the $^{52}Cr/^{53}Cr$ ratio of the sample/spike mixture measured by inductively couple plasma mass spectrometry (ICP-MS; Thermo Scientific Element 2). CrT values measured by the single and double spike methods were generally within 2-5% of one another, although in one instance the difference was 8%. Only double spike CrT values are reported in Section 4 as the precision of this technique was superior (typically 0.5-2% for single spike data, and <0.05% for double spike data).

3.2.2 Preparation of seawater samples for Cr isotope analysis

As the Cr content of seawater is relatively low, it was necessary to pre-concentrate the Cr by co-precipitation with Fe using a modified version of the method described in Bonnand et al. 2013. First, 30-70 µg of a ^{50}Cr-^{54}Cr double spike (2.78 ppm) was added to between 1 and 2 L of seawater (~150 to 300 ng of natural Cr). In order to reduce the error magnification term associated with isotopic ratio measurements (Bonnand et al., 2011), optimal target ratios were set for $^{50}Cr/^{52}Cr$, $^{53}Cr/^{52}Cr$ and $^{54}Cr/^{52}Cr$ (Table 3). The exact amount of double spike added to each sample was calculated based on individual sample weights and concentrations (as estimated by single spike ID; Section 3.2.1). The double spike was dispensed into the sample using a variable volume pipette calibrated with Milli-Q water (n=5, 2SD = ±0.0001 – 0.0005 g), and the weight of spike added to each sample was calculated from the mass dispensed multiplied by the density of the double spike (1.0980 g mL-1). The sample-spike mixtures were then left to equilibrate for ~24 hours. The Cr in the double spike is present as Cr(III), which is expected to be the principal Cr species in acidified (pH 2) samples (Rai et al. 1989). For this reason equilibration between spike and sample Cr was expected to be rapid.

After ~24 hours, samples were adjusted to pH 8-9 to facilitate precipitation of Cr, and a freshly prepared suspended precipitate of Fe(II) hydroxide (made by the addition of ammonia to a fresh ammonium Fe(II) sulphate solution) was added (10 ml L-1 of seawater). Under these conditions, any remaining Cr(VI) in the sample is quantitatively reduced to Cr(III) by Fe(II) (Fendorf and Li, 1996), which is in turn oxidised to Fe(III), forming an Fe(III)-Cr(III) precipitate. Chromium(III) is quantitatively adsorbed onto the Fe(III)-Cr(III) precipitate (Crawford et al., 1993), ensuring that all of the Cr in the sample is recovered.

The precipitate was separated from the solution via vacuum filtration through Millipore Omnipore filters (1 μm), which were pre-cleaned in 6 M sub-boiled HCl at 95°C followed by Milli-Q water at 95°C (Scheiderich et al., 2015). The precipitate was then leached from the filters using 6M HCl before being dried down and taken up in 6 mL of 7 M HCl. The Cr was separated from the Fe via anion exchange chromatography (Biorad AG1-X8, 200-400 mesh size; Bonnand et al. 2013), and the eluant was then dried and re-dissolved in 6 mL of 0.5 M HCl. Remaining cations were removed by cation exchange chromatography (Biorad AG50-X12, 200-400 mesh size; Bonnand et al. 2011). The eluant was then dried down and 30 μL H_2O_2 was added before the solution was dried down once again in order to oxidise any remaining organic material. This step was found to prevent a loss of ion beam intensity during analysis, which is thought to be caused by interaction between residual organic material and the sampling probe and/or the Aridus 2 nebuliser system (see below).

3.2.3 MC-ICP-MS analysis

Cr isotopic values and concentrations were measured at the University of Southampton using a method similar to that described in Bonnand et al. 2011. Samples were introduced to a Thermo Fisher Neptune MC-ICP-MS using an Aridus 2 desolvating nebuliser system with argon (Ar) as the carrier gas (operational settings can be found in Table 4). Nitrogen was omitted to reduce the size of ArN+ polyatomic interferences. The intensities of the four naturally occurring stable isotopes of Cr (^{50}Cr, ^{52}Cr, ^{53}Cr, ^{54}Cr) were measured in addition to ^{49}Ti, ^{51}V and ^{56}Fe in order to correct for isobaric interferences from ^{50}Ti, ^{50}V and ^{54}Fe. Medium resolution settings and 1011 Ω resistors were used and a gain calibration was also performed before each analytical session. A baseline correction was carried out at the beginning of each measurement. Polyatomic interferences such as $^{40}Ar^{14}N+$ and $^{40}Ar^{16}O+$ were avoided by making measurements on the peak shoulders.

The signal intensity of ^{52}Cr for a double spiked 50 ppb Cr solution with these settings was ~6-7V. The signal intensity of the samples was always within ~10% of this solution. Each analytical session began with analysis of at least three spiked NBS979 standards to verify instrument performance, followed by analysis of one spiked NBS979 standard after every three samples. The blank solution (3% HNO_3) was measured before and after each sample or standard, and the signal intensities were subtracted from the sample/standard data. A Newton-Raphson deconvolution calculation was performed to extract the $\delta^{53}Cr$ value of the sample (Albarède and Beard, 2004). Whilst the double spike corrects for instrumental mass bias

effects, instrumental drift that arises due to variable collection efficiency of the Faraday cups over multiple analytical sessions must still be accounted for. This was done by normalising $\delta 53Cr$ values to the daily average $\delta 53Cr$ value for the NBS979 standard reference material.

4. Results

4.1 Method validation

The Cr blank for the Fe(II) co-precipitation method was 18 ± 0.9 ng, the majority of which (~93%) was contributed by the ammonium Fe(II) sulphate salt (Sigma-Aldrich) used to generate the Fe(II) hydroxide precipitate. The isotopic composition of the trace amount of Cr in this salt varied slightly between batches, possibly due to an uneven distribution of isotopes within the crystals. For this reason, the CrT and $\delta 53Cr$ of the ammonium Fe(II) sulphate solution was regularly determined (respectively, 16.68 ± 0.55 nmol kg-1, -0.34 ± 0.32‰ 2SD, n=6) and corrections to the final data were applied to account for its contribution to CrT and $\delta 53Cr$ of the samples. Uncertainty in the Cr concentration of the Fe(II) solution (together with the minor uncertainty of the volume of Fe(II) solution added to the sample) contributed an uncertainty of ± 0.005 nmol kg-1 in corrected sample CrT values, yielding an external reproducibility of 0.03 nmol kg-1 (2SD). The effect of the blank on the uncertainty of $\delta 53Cr$ was ± 0.02‰ (2SD), but it is higher (± 0.04‰) for samples with heavier $\delta 53Cr$ values (>1.6‰). The uncertainty of the seawater processing method based on 6 analyses of the OSIL salinity standard using the same Fe(II) solution was ± 0.10‰ (Table 5). Propagation of these uncertainties yields an external reproducibility value of better than ± 0.11‰ (2SD) for our seawater samples, which is slightly higher than the reproducibility of our normalised NBS979 standards (± 0.04‰, n=214; Figure 2).

Despite the large quantities of Fe added to the samples during co-precipitation, efficient removal of Fe by anion exchange chromatography ensured that the 56Fe/54Cr of the samples was always <0.50 and usually around 0.03. Several Fe doped NBS979 standards were tested to confirm that accurate $\delta 53Cr$ values could be retrieved by the double spike procedure for 56Fe/54Cr ratios of between 0.02 and 0.50. These solutions produced an average $\delta 53Cr$ value of -0.01 ± 0.04‰ (2SD, n=35), within error of NBS979 standards containing no additional Fe (0.00 ± 0.04‰, n=214) indicating that 56Fe/54Cr ratios of up to 0.5 could be successfully tolerated.

In the absence of a seawater Cr isotope standard, several tests were carried out to evaluate the accuracy of the method. First, a standard addition experiment was performed using a

seawater sample from Southampton Water mixed with the NBS979 Cr standard. Southampton Water is ideal for this purpose as it has a relatively heavy $\delta^{53}Cr$ value (Bonnand et al., 2013) compared to NBS979, allowing a wide range of standard-seawater $\delta^{53}Cr$ values to be tested. The relationship between measured $\delta^{53}Cr$ and the proportion of seawater present was linear, with a gradient (0.014) similar to that expected from mixing calculations (0.015; Figure 3). Furthermore a negligible offset from 0‰ for NBS979 is predicted by the y-intercept of the graph (0.02 ± 0.03‰). This indicates that accurate $\delta^{53}Cr$ measurements are achievable for the entire range of seawater values (0.13 - 1.72‰; Bonnand et al. 2013; Scheiderich et al. 2015; Paulukat et al. 2016; this study).

In order to confirm that the $\delta^{53}Cr$ composition of the NBS979 standard could be replicated for a seawater matrix, as predicted by the standard addition experiment, 500mL of OSIL seawater was doped with 10μg of NBS979 such that the contribution of seawater Cr to the OSIL-NBS979 mixture was negligible. The solution was split into 5 aliquots and these were processed separately. The average $\delta^{53}Cr$ value was 0.03 ± 0.02‰ (2SD), within error of the value predicted by the y-intercept of the standard addition experiment and very close to the true $\delta^{53}Cr$ value of NBS979 (0‰). Given that the external reproducibility of our seawater analyses is ±0.11‰ for the seawater method, this indicates that the NBS979 standard behaves in the same way as seawater during processing. The concentration of this solution was determined to be 360.4 ± 0.1 nmol kg-1 (2SD), which was within 0.4% of the expected value (359.1 nmol kg-1).

Finally, the CrT and $\delta^{53}Cr$ values that we measured for Southampton Water and the OSIL Atlantic Salinity Standard seawater (Table 5) were within error of previously published values with the exception of the CrT of Southampton Water. The Southampton Water sample used in this study was different from that used in a previous study (Bonnand et al., 2013) and had a lower salinity (30 versus 34), so additional river water input with low CrT could account for the lower CrT in the sample (though the CrT values of the contributing rivers are unknown). Overall, these validation experiments show that the Fe(II) co-precipitation method produces accurate results for seawater samples, with comparable precision to previously published seawater values.

4.2 CrT and $\delta^{53}Cr$ in the eastern tropical Atlantic Ocean

The distribution of salinity along a section at 12°N that encompasses all of the shelf and slope stations sampled on cruise D361 (stations 2-5) is shown in Figure 4A. The Guinea Dome can

be identified by the doming of isohalines in the surface waters around 22°W and the mixing of shelf and open ocean waters can be seen between 0-300m, 18-20°W. Profiles of salinity (Figure 4B) for stations 18 and 11.5 show sub-surface salinity maxima that originate from Tropical Surface Water and South Atlantic waters, respectively. These salinity maxima are overlain by low-salinity equatorial sourced waters which have experienced high levels of precipitation (Stramma et al., 2005). The SACW has variable salinity whereas the salinity of AAIW and NADW is consistent across all stations except for 11.5, where the AAIW salinity minimum is more prominent because the water mass has travelled less far from its source and has experienced less mixing (Figures 4B+C).

Concentrations of O2 within the OMZ were higher than those typically measured within the eastern tropical Pacific (~15 µmol kg-1) and northern Indian Ocean (~13-16 µmol kg-1) OMZs (Paulmier and Ruiz-Pino, 2009). The core of the OMZ was at ~450m for the slope stations 2 and 3, and for open ocean station 18 (Figure 5). The lowest OMZ O2 concentrations (44-51 µmol kg-1) were found at stations 2, 3 and 18. At shelf stations 4 and 5 the lowest O2 concentrations (66-93 µmol kg-1) were found closest to the sea bed, as upwelling supplied waters that were already somewhat oxygen depleted and there was no ventilation from deeper water masses. At Station 11.5 the OMZ had a higher O2 concentration (90-100 µmol kg-1) and there was a secondary, smaller O2 minimum at 1000-1300m due to the presence of UCDW. Chlorophyll-a (Chl-a) concentrations of up to 2.1mg m-3 were recorded on the slope where upwelling actually occurs, indicating high phytoplankton biomass levels. Concentrations of up to 1.5 mg m-3 were also observed on the shelf itself. Away from the upwelling area Chl-a concentrations were much lower (≤0.5mg m-3; Figure 5).

Profiles of CrT and δ53Cr are presented in Figures 6 and 7 (see Table 6 for all data). Seawater δ53Cr values ranged from 1.08 to 1.72‰, similar to or slightly higher than previously published values (0.13 to 1.55‰; Bonnand et al. 2013; Paulukat et al. 2015; Pereira et al. 2015; Scheiderich et al. 2015; Economou-Eliopoulos et al. 2016; Holmden et al. 2016; Paulukat et al. 2016). The CrT showed only limited variation, ranging from 2.1 to 2.9 nmol kg-1, which is within the range previously measured for seawater (0.9-6.5 nmol kg-1; Campbell and Yeats 1981; Cranston 1983; Jeandel and Minster 1984; Achterberg and Berg 1997; Sirinawin et al. 2000; Connelly et al. 2006; Bonnand et al. 2013; Scheiderich et al. 2015). The concentrations of CrT at the open ocean stations (stations 11.5 and 18) occupied the higher end of the range (2.5-2.9 nmol kg-1).

Relatively heavy δ53Cr values were present at all depths at shelf stations 4 and 5 (1.21-1.62‰), and on average CrT was 15% lower at these two stations compared to slope and open ocean stations (stations 2, 3, 11.5 and 18). At the slope stations 2 and 3, intermediate δ53Cr and CrT values were found in the top 300m compared to shelf and open ocean stations. This represents mixing of open ocean and shelf Cr as high salinity shelf waters mixed with deeper, lower salinity waters at 18-20°W (Figures 4 and 8A). Within the OMZ at 400-500m water depth, station 2 had a distinct δ53Cr maximum (1.71‰), while there was little change in δ53Cr at station 3, despite similar O2 concentrations at both stations. At open ocean stations 11.5 and 18, the δ53Cr range was quite narrow throughout the water column (1.08 to 1.26‰) with the exception of one sample from within UCDW at station 11.5 which had notably higher δ53Cr (1.72‰).

5. Discussion

Our CrT and δ53Cr data are compared with all other available data for seawater in Figure 9. Most of our data cluster close to the 'global correlation' line defined for seawater samples that has been interpreted to reflect reduction of Cr(VI) in surface waters and OMZs, coupled with re-oxidation of Cr(III) in deep waters (Scheiderich et al., 2015). Considered by themselves, however, there is no correlation ($R^2 = 0.12$) between lnCrT and δ53Cr for seawater samples from the eastern tropical Atlantic Ocean; the range of δ53Cr is relatively large and the range of CrT is relatively low compared to seawater samples collected from other parts of the ocean.

5.1 CrT and δ53Cr in the OMZ at the slope and open ocean stations

There was no correlation between concentrations of CrT or δ53Cr values and dissolved oxygen for seawater from the slope (stations 2 and 3) and open ocean (stations 11.5 and 18) (Figures 8B and 8D). This suggests either that reduction of Cr(VI) to Cr(III) is insignificant in the offshore part of the eastern Atlantic OMZ, or that reduction of Cr(VI) to Cr(III) occurs but, because particle concentrations (measured by light transmissometry) at these stations are low (Figure 8C), any Cr(III) that forms is not adsorbed on particles and subsequently removed from the CrT pool. Concentrations of nitrite were negligible within the OMZ (<0.01 μmol L-1; data including analytical methodologies available on request from the British Oceanographic Data Centre, www.bodc.ac.uk), indicating that nitrate reduction did not occur. As nitrate and Cr(VI) (in the form of chromate, CrO_4^{2-}) have similar standard electrode potentials ($CrO_4^{2-}/Cr(OH)_3$ = -0.12V, NO_3^-/NO_2^- = 0.01V; Bratsch 1989, Fanning 2000),

we suggest that it is most likely that reduction of Cr(VI) only occurs in waters with much lower levels of dissolved oxygen.

The amount of remineralised CrT in the water column between 100 m and 1000 m depth can be estimated from the apparent oxygen utilisation (AOU), assuming an AOU/C ratio of 1.6 (Martin et al., 1987) and a Cr/C ratio of 10 µmol Cr/mol C, which is at the lower end of reported Cr/C ratios for marine particles with a high biogenic component (10-300 µmol Cr/mol C; Dauby et al., 1994) but higher than cellular Cr/C ratios for marine phytoplankton (<0.5 µmol Cr/mol C; Semeniuk et al., 2016). Whatever value of Cr/C is used, the contribution of remineralised Cr to the total Cr concentration is similar for all stations and there is no relationship between the proportion of remineralised Cr and CrT or $\delta53Cr$; changes in the proportion of remineralised Cr are principally driven by AOU. By contrast, the contribution of remineralised Fe to the total dFe pool increases from the shelf (stations 4 and 5) to the slope (stations 2 and 3), and there is a strong correlation between the proportion of remineralised Fe and $\delta56Fe$ that indicates that remineralised Fe has a distinct iron isotopic signature (Klar et al., this issue). Remineralisation of organic material within the OMZ therefore does not appear to be a significant source of CrT.

The deep (>1000 m) water masses sampled from slope station 2 and open ocean stations 11.5 and 18 have a similar range of $\delta53Cr$ values (1.27 ± 0.21‰; 1SD) to surface and sub-surface waters (1.27 ± 0.16‰), thus there is no evidence for input of Cr from re-oxidation of Cr(III) in the deep waters. The AAIW has slightly higher CrT compared to NADW, with CrT values ranging from 2.48-2.71 nmol kg-1 and $\delta53Cr = 1.16 \pm 0.06$‰ (1SD, n=8) at Stations 2, 3 and 18 (all at ~12°N). CrT and $\delta53Cr$ values for AAIW are higher at station 11.5 (at 3°S; 2.90 nmol kg-1, 1.21‰ respectively). This probably reflects a 'purer' AAIW signal as the water mass is less attenuated at this site. Average CrT and $\delta53Cr$ values for the NADW (sampled at stations 2, 18 and 11.5, n=7) are also similar (2.61 ± 0.13 nmol kg-1, 1.21 ± 0.12‰, 1SD). The deepest samples taken from stations 2 and 18 have slightly higher CrT than the other NADW samples that may reflect mixing with AABW (Station 18) and/or input of benthic sedimentary Cr (both stations). Our results are comparable with those for other intermediate and deep Atlantic water masses (1.15‰ for Atlantic Water and 1.06‰ for Canada Basin Deep Water; Scheiderich et al. 2015), but water samples recovered from the Argentine Basin have lower $\delta53Cr$ values (0.41 to 0.66‰; Bonnand et al., 2013). The Argentine Basin samples were not filtered as concentrations of suspended particulate material were thought to be low; if Cr was leached from particulate material then this would likely reduce the $\delta53Cr$

value of the dissolved fraction (e.g. crustal rocks have δ53Cr = -0.12 ± 0.10‰; Schoenberg et al. 2008).

Two of the seawater samples from the slope and open ocean stations have relatively high δ53Cr values (~1.7‰) that deviate from the 'global correlation' line shown in Figure 9. One of these was collected from ~400m water depth within the OMZ at station 2, while the other was collected from within UCDW at ~1100m water depth at station 11.5. The sample from station 2 had unusually low dFe compared to other samples from within the OMZ (Figure 10; Klar et al. this issue). Low dFe and high δ53Cr would be consistent with reduction of Cr(VI) in the presence of Fe(II), followed by the removal of the resulting Fe(III)-Cr(III) precipitate. However, there is no evidence for removal of Cr(III) as CrT is slightly enhanced at this depth. One other potential explanation is the injection of higher salinity waters (that originate from the surface and thus have low dFe and high δ53Cr) at this depth (Figure 4). Sub-surface currents at this location are complex due to upwelling at the shelf break region and in the Guinea Dome region, and due to interactions with the equatorial current system (Stramma et al., 2005), such that upper SACW has variable salinity.

The sample from ~1100 m at station 11.5 was the only sample taken from within UCDW. Its relatively heavy δ53Cr value may simply represent the pre-formed signature of this water mass. The δ53Cr values of ICW and SPCW source waters that form UCDW have not yet been measured, but these water masses both experience oxygen depletion prior to their incorporation into UCDW (Gordon et al., 1992; Karstensen and Tomczak, 1997; Tomczak and Godfrey, 2003; Kawabe and Fujio, 2010). It is possible that this has led to partial reduction of Cr(VI), enriching residual Cr in heavy Cr isotopes. The only other reported δ53Cr value for UCDW was from the Argentine Basin, and is substantially lower (0.52‰; Bonnand et al. 2013). This may, however, be due to differences in sample processing procedures (see above).

5.2 Benthic supply of Cr on the Senegalese shelf

On the shelf (stations 4 and 5), CrT concentrations and δ53Cr values were slightly higher in the deeper dysoxic waters than they were in the upper oxic waters and there are significant negative correlations between CrT, δ53Cr and dissolved O2 (respectively, p < 0.01 and p <0.1; Figures 8B and 8D). While reduction of Cr(VI) is expected to increase the δ53Cr of remaining Cr(VI) (Sikora et al., 2008; Zink et al., 2010; Døssing et al., 2011; Kitchen et al., 2012), this process would also be expected to lower CrT concentrations if the Cr(III) that

forms is adsorbed onto particles (Scheiderich et al. 2015) which are abundant on the shelf (Figure 8C). Moreover, the shelf waters with highest CrT also have relatively high $\delta^{53}Cr$ (1.4 - 1.6‰). This is inconsistent with release of Cr(III) from biogenic material during remineralisation of organic matter (Dauby et al., 1994; Connelly et al., 2006; Semeniuk et al., 2016) as Cr(III) is expected to be enriched in light Cr isotopes (Scheiderich et al., 2015; Semeniuk et al., 2016).

Although concentrations of CrT on the shelf are lower than they are on the slope and in the open ocean, increased levels of CrT in the bottom waters are nevertheless consistent with input of Cr from shelf sediments. Concentrations of CrT are positively correlated with concentrations of dissolved iron (dFe) ($R^2 = 0.88$, $p < 0.0005$; Figure 8E). The seawater samples that have high dFe also have relatively low $\delta^{56}Fe$ values (down to -0.3‰) that is, in part, due to input of pore waters that are enriched in Fe produced by dissimilatory iron reduction (DIR) within the sediments (Klar et al., this issue). Accordingly, $\delta^{56}Fe$ is negatively correlated with CrT ($R^2 = 0.52$, $p < 0.05$) and $\delta^{53}Cr$ ($R^2 = 0.30$, $p < 0.15$; Figure 8F). We suggest that if the oxic/suboxic front is located at or very close to the sediment-seawater interface on the shelf, then Cr released from sediments by oxidation at the front may be partly back-reduced within the sediments (for example by organic molecules; Jamieson-Hanes et al., 2012; Kitchen et al., 2012), enriching the residual Cr(VI) in heavy Cr isotopes. Oxidation of upward diffusing Fe(II) at some depth below the front would, by contrast, further enrich residual Fe(II) in light isotopes (Severmann et al., 2006; Homoky et al., 2009). Part of the Fe(II) may escape oxidation as it is stabilised by complexation by dissolved organic material (Klar et al., 2017; Klar et al., this issue). In support of this, Cr release to sediment pore waters and into the overlying water column was observed in association with Fe oxyhydroxide reduction in the Berre Lagoon (France; Rigaud et al. 2013), and analyses of Cr concentrations in pore waters of the California Margin revealed that Cr is mobilised from sediments at the oxic/suboxic front in shelf sediments (Shaw et al., 1990).

5.3 Removal of Cr in shelf waters?

Concentrations of CrT were slightly lower on the shelf (2.21 ± 0.07 nmol kg-1) than in open ocean waters at the same water depth (between 0 and 160m, 2.48 ± 0.07 nmol kg-1). The shelf waters also had higher $\delta^{53}Cr$ values (1.41 ± 0.14‰ compared to 1.18 ± 0.05‰ for open ocean waters shallower than 160m). Arctic shelf waters and coastal water from Southampton Water (UK) also have relatively high $\delta^{53}Cr$ and low CrT values (Bonnand et al., 2013;

Scheiderich et al., 2015) and are thought to be affected by local inputs of river water and, in the case of the Arctic, melting sea ice.

Stations 4 and 5 are located >80 km from the coast and are not affected by local fresh water inputs. However, concentrations of Chl-a in shelf waters are high, and light transmittance is low, indicating that, respectively, levels of primary productivity and particle concentrations are high (Figures 5 and 8C). Laboratory experiments have shown that a variety of marine phytoplankton and algae (Li et al., 2009) as well as microbes (Sikora et al., 2008), can reduce Cr(VI). This raises the possibility that the low CrT and high $\delta^{53}Cr$ values on the Senegalese shelf reflect partial reduction of Cr(VI), with subsequent removal of the relatively isotopically light Cr(III) that forms onto particle surfaces (Scheiderich et al., 2015). Reduction of Cr(VI) in the surface ocean may also be promoted by photochemical reactions that produce Cr reductants such as H_2O_2 and Fe(II) (Pettine and Millero, 1990; Li et al., 2009).

No water samples were collected from within the sub-surface Chl-a maxima at the slope stations (2 and 3), but samples from within the Chl-a maxima at the open ocean stations (11.5 and 18) do not have relatively low CrT and high $\delta^{53}Cr$ values as we found on the shelf. This does not necessarily imply that reduction of Cr(VI) does not occur in surface waters (via biological or photochemical processes); rather, the absence of significant concentrations of particles that is implied by high light transmittance readings (Figure 8C) may mean that any Cr(III) that is produced is simply not removed from the CrT pool. To assess this, analyses of Cr(III) and Cr(VI) concentrations, and analyses of the Cr isotopic compositions of the individual Cr(III) and Cr(VI) pools, are required.

5.4 Input of Cr from atmospheric sources

Atmospheric dust has previously been shown to affect Cr concentrations in surface waters of the Mediterranean Sea (Achterberg and Berg, 1997). The $\delta^{53}Cr$ value of this potential Cr source is unknown but, assuming that Cr isotopes are not fractionated during dissolution, it is likely to be similar to the $\delta^{53}Cr$ value of crustal rocks (-0.12 ± 0.10‰; Schoenberg et al. 2008). Based on concentrations of dissolved aluminium (dAl) within the surface mixed layer (SML), the annual flux of dust delivered to the shelf (stations 4 and 5) was estimated to be ~0.019 g m-2, whereas in the open ocean it varied from ~2.8 g m-2 at station 18 to ~1.2 g m-2 at station 11.5 (Klar et al., this issue); station 11.5 is shielded from dust input by the inter-tropical convergence zone (Schlosser et al., 2014). We note that there is little difference in

CrT in the SML between the two open ocean sites (station $11.5 = 2.41$ nmol kg-1 and station $18 = 2.48$ nmol kg-1 at 24 and 29m respectively), even though the dust input to station 11.5 is substantially lower than it is at station 18. This implies that dust inputs are not a significant source of Cr to the (sub)-tropical east Atlantic Ocean.

5.5 Implications for the $\delta^{53}Cr$ redox proxy

Several studies have used the $\delta^{53}Cr$ composition of authigenic marine sediments to decipher past changes in atmospheric and seawater oxygenation (Frei et al., 2009; Crowe et al., 2013; Planavsky et al., 2014; D'Arcy et al., 2016; Gilleaudeau et al., 2016). For example, $\delta^{53}Cr$ values in banded iron formations (BIFs) have been interpreted to preserve the $\delta^{53}Cr$ value of overlying seawater assuming that Cr(VI) is quantitatively reduced in the presence of Fe minerals, and the Cr(III) that forms is incorporated into the BIFs (Frei et al., 2009). Thus BIFs that have relatively high $\delta^{53}Cr$ have been interpreted to capture relatively high seawater $\delta^{53}Cr$ values that are characteristic of oxidative weathering, whereas $\delta^{53}Cr$ values close to those of crustal rocks (-0.12 ± 0.10‰; Schoenberg et al. 2008) were suggested to indicate the absence of oxidative weathering, and thus low atmospheric O_2 (Frei et al., 2009; Crowe et al., 2013; Frei et al., 2013; Planavsky et al., 2014).

Our new data, together with existing data, indicate that seawater has an average $\delta^{53}Cr$ value of 1.16 ± 0.27‰ (1SD, n=99), though the range of values is larger for surface waters (Figure 11). The $\delta^{53}Cr$ values of authigenic phases within anoxic (euxinic) marine sediments from the Cariaco Basin in the Atlantic Ocean (0.4 ± 0.1‰) have been interpreted to reflect the $\delta^{53}Cr$ value of overlying seawater (Reinhard et al., 2014; Gueguen et al., 2016). Although no $\delta^{53}Cr$ data are available for seawater in the Cariaco Basin, we suggest that this is unlikely given that there is little overlap between seawater and authigenic phase $\delta^{53}Cr$ values. Rather, we suggest that Cr is not quantitatively reduced under anoxic conditions, such that the $\delta^{53}Cr$ of the Cr(III) incorporated in sediments is lower than the $\delta^{53}Cr$ value of seawater; this is supported by a study of the Saanich Inlet that showed that significant concentrations of Cr(III) and Cr(VI) persist in anoxic waters (Emerson et al., 1979).

Our data also indicate that the Cr isotopic composition of seawater may not simply reflect the $\delta^{53}Cr$ value of the river input as it can also be affected by the Cr cycling within the ocean, especially in shelf settings. The range in $\delta^{53}Cr$ values in the eastern sub-tropical Atlantic ocean ranges from 1.08 to 1.72‰, and variations can principally be attributed to (i) reduction of Cr(VI) and uptake of Cr(III) on particles and (ii) input of benthic sedimentary Cr. Thus

relatively subtle changes in δ53Cr of authigenic marine precipitates, of the order of that reported for the authigenic fraction of sediments from the Peru Margin (~0.6-0.7‰; Gueguen et al., 2016), may occur independently of changes in seawater oxygenation. On the other hand, our eastern sub-tropical Atlantic seawater data reveal that the δ53Cr values of AAIW and NADW are remarkably consistent (1.19 ± 0.09‰), such that changes in δ53Cr of authigenic phases that form in open ocean settings may reliably record variations in seawater δ53Cr that can be interpreted in terms of changes in Cr inputs to the ocean.

6. Conclusions

We found that oxygen concentrations as low as 44 μmol kg-1 within the eastern equatorial Atlantic Ocean OMZ had no systematic effect on δ53Cr values or CrT on the Senegalese slope and in the open ocean. Inputs of Cr from remineralisation of organic material, re-oxidation of Cr(III) in deep waters, and atmospheric dust also appeared to be minimal in the slope and open ocean waters. By contrast, waters on the Senegalese shelf had relatively high δ53Cr values and low CrT compared to the slope and open ocean waters, coinciding with high levels of biological productivity and high concentrations of suspended particulate material on the shelf. Our δ53Cr and CrT data are consistent with reduction of Cr(VI) (by either biological or photochemical processes) and uptake of the Cr(III) that forms onto particles. The deeper, dysoxic shelf waters have higher CrT concentrations and relatively heavy δ53Cr values that point to release of Cr from sediments.

Considered together with all other published Cr isotope data for seawater, the average δ53Cr value for seawater is 1.16 ± 0.27‰, and δ53Cr is independent of the concentration of dissolved oxygen, at least for oxic and dysoxic waters. Thus relatively small changes in δ53Cr values of ancient marine authigenic precipitates may not necessarily reflect past changes in levels of dissolved oxygen in seawater, or atmospheric oxygenation.

References

Abu-Saba, K.E. and Flegal, A.R. (1995) Chromium in San Francisco Bay: superposition of geochemical processes causes complex spatial distributions of redox species. Mar. Chem. 49, 189-199.

Abu-Saba, K.E. and Flegal, A.R. (1997) Temporally variable freshwater sources of dissolved chromium to the San Francisco Bay estuary. Environ. Sci. Technol. 31, 3455-3460.

Achterberg, E.P. and Berg, C.M.G.v.d. (1997) Chemical speciation of chromium and nickel in the western Mediterranean. Deep Sea Res. (II Top. Stud. Oceanogr.) 44, 693-720.

Albarède, F. and Beard, B. (2004) Analytical methods for non-traditional isotopes. Reviews in Mineralogy & Geochemistry 55, 113-152.

Bain, D.J. and Bullen, T.D. (2005) Chromium isotope fractionation during oxidation of Cr(III) by manganese oxides. Geochim. Cosmochim. Acta 69.

Basu, A., Johnson, T.M. and Sanford, R.A. (2014) Cr isotope fractionation factors for Cr(VI) reduction by a metabolically diverse group of bacteria. Geochim. Cosmochim. Acta 142, 349-361.

Bedson, P. (2007) Guidelines for achieving high accuracy in isotope dilution mass spectrometry (IDMS). Royal Society of Chemistry, Cambridge, GBR.

Berger, A. and Frei, R. (2014) The fate of chromium during tropical weathering: A laterite profile from Central Madagascar. Geoderma 213, 521-532.

Bonnand, P., James, R.H., Parkinson, I.J., Connelly, D.P. and Fairchild, I.J. (2013) The chromium isotopic composition of seawater and marine carbonates. Earth. Planet. Sci. Lett. 382, 10-20.

Bonnand, P., Parkinson, I.J., James, R.H., Karjalainena, A.-M. and Fehra, M.A. (2011) Accurate and precise determination of stable Cr isotope compositions in carbonates by double spike MC-ICP-MS. J. Anal. At. Spectrom. 26, 528-535.

Bratsch, S.G. (1989) Standard Electrode Potentials and Temperature Coefficients in Water at 298.15K. J. Phys. Chem. Ref. Data 18, 1-21.

Campbell, J.A. and Yeats, P.A. (1981) Dissolved chromium in the northwest Atlantic Ocean. Earth. Planet. Sci. Lett. 53, 427-433.

Chester, R. and Murphy, K.J.T. (1990) Metals in the marine atmosphere, in: Furness, R., Rainbow, P. (Eds.), Heavy Metals in the Marine Environment. CRC Press, Boca Raton, FL, pp. 27-49.

Connelly, D.P., Statham, P.J. and Knap, A.H. (2006) Seasonal changes in speciation of dissolved chromium in the surface Sargasso Sea. Deep Sea Res. (I Oceanogr. Res. Pap.) 53, 1975-1988.

Cranston, R.E. (1983) Chromium in Cascadia Basin, northeast Pacific Ocean. Mar. Chem. 13, 109-125.

Cranston, R.E. and Murray, J.W. (1980) Chromium species in the Columbia River and estuary. Limnol. Oceanogr. 25, 1104-1112.

Crawford, R.J., Harding, I.H. and Mainwaring, D.E. (1993) Adsorption and coprecipitation of single heavy metal ions onto the hydrated oxides of iron and chromium. Langmuir 9, 3050-3056.

Crowe, S.A., Døssing, L.N., Beukes, N.J., Bau, M., Kruger, S.J., Frei, R. and Canfield, D.E. (2013) Atmospheric oxygenation three billion years ago. Nature 535-539.

D'Arcy, J., Gilleaudeau, G.J., Peralta, S., Gaucher, C. and Frei, R. (2016) Redox fluctuations in the Early Ordovician oceans: An insight from chromium stable isotopes. Chem. Geol 448, 1-12.

D'Arcy, J., Babechuk, M.G., Døssing, L.N., Gaucher, C. and Frei, R. (2016) Processes controlling the chromium isotopic composition of river water: Constrains from basaltic river catchments. Geochim. Cosmochim. Acta 186, 296-315.

Dauby, P., Frankignoulle, M., Gobert, S. and Bouquegnou, J. (1994) Distribution of POC, PON, and particulate Al, Cd, Cr, Cu, Pb, Ti, Zn and 813C in the English Channel and adjacent areas. Oceanol. Acta 17, 643-657.

Dolamore-Frank, J.A. (1984) The analysis, occurrence and chemical speciation of zinc and chromium in natural waters. University of Southampton, UK.

Døssing, L.N., Dideriksen, K., Stipp, S.L.S. and Frei, R. (2011) Reduction of hexavalent chromium by ferrous iron: A process of chromium isotope fractionation and its relevance to natural environments. Chem. Geol. 285, 157-166.

Economou-Eliopoulos, M., Frei, R. and Megremi, I. (2016) Potential leaching of Cr(VI) from laterite mines and residues of metallurgical products (red mud and slag): An integrated approach. Journal of Geochemical Exploration 162, 40-49.

Elderfield, H. (1970) Chromium speciation in seawater. Earth. Planet. Sci. Lett. 9, 10-16.

Ellis, A.S., Johnson, T.M. and Bullen, T.D. (2002) Chromium isotopes and the fate of hexavalent chromium in the environment. Science 295, 2060-2062.

Emerson, S., Cranston, R.E. and Liss, P.S. (1979) Redox species in a reducing fjord: equilibrium and kinetic considerations. Deep Sea Research Part A. Oceanographic Research Papers 26, 859-878.

Fanning, J.C. (2000) The chemical reduction of nitrate in aqueous solution. Coord. Chem. Rev. 199, 159-179.

Fendorf, S.E. and Li, G. (1996) Kinetics of Chromate Reduction by Ferrous Iron. Environ. Sci. Technol. 30, 1614-1617.

Frei, R., Gaucher, C., Poulton, S.W. and Canfield, D.E. (2009) Fluctuations in Precambrian atmospheric oxygenation recorded by chromium isotopes. Nature 461, 250-253.

Frei, R., Gaucher, C., Stolper, D. and Canfield, D.E. (2013) Fluctuations in late Neoproterozoic atmospheric oxidation — Cr isotope chemostratigraphy and iron speciation of the late Ediacaran lower Arroyo del Soldado Group (Uruguay). Gondwana Res 23, 797-811.

Frei, R., Poiré, D. and Frei, K.M. (2014) Weathering on land and transport of chromium to the ocean in a subtropical region (Misiones, NW Argentina): A chromium stable isotope perspective. Chem. Geol. 381, 110-124.

Frei, R. and Polat, A. (2013) Chromium isotope fractionation during oxidative weathering— Implications from the study of a Paleoproterozoic (ca. 1.9 Ga) paleosol, Schreiber Beach, Ontario, Canada. Precambrian Res. 224, 434-453.

Gaillardet, J., Viers, J. and Dupré, B. (2003) 5.09 - Trace elements in river waters, in: Holland, H.D., Turekian, K.K. (Eds.), Treatise on Geochemistry. Pergamon, Oxford, pp. 225-272.

Gardner, M.J. and Ravenscroft, J.E. (1996) Determination of chromium(III) and total chromium in marine waters. Fresenius J. Anal. Chem. 354, 602-605.

Gilleaudeau, G.J., Frei, R., Kaufman, A.J., Kah, L.C., Azmy, K., Bartley, J.K., Chernyavskiy, P. and Knoll, A.H. (2016) Oxygenation of the mid-Proterozoic atmosphere: clues from chromium isotopes in carbonates. Geochemical Perspectives Letters 2, 179-187.

Gordon, A.L., Weiss, R.F., Smethie, W.M. and Warner, M.J. (1992) Thermocline and intermediate water communication between the south Atlantic and Indian oceans. Journal of Geophysical Research: Oceans 97, 7223-7240.

Gueguen, B., Reinhard, C.T., Algeo, T.J., Peterson, L.C., Nielsen, S.G., Wang, X., Rowe, H. and Planavsky, N.J. (2016) The chromium isotope composition of reducing and oxic marine sediments. Geochim. Cosmochim. Acta 184, 1-19.

Helly, J.J. and Levin, L.A. (2004) Global distribution of naturally occurring marine hypoxia on continental margins. Deep Sea Research Part I: Oceanographic Research Papers 51, 1159-1168.

Holmden, C., Jacobson, A.D., Sageman, B.B. and Hurtgen, M.T. (2016) Response of the Cr isotope proxy to Cretaceous Ocean Anoxic Event 2 in a pelagic carbonate succession from the Western Interior Seaway. Geochim. Cosmochim. Acta 186, 277-295.

Izbicki, J.A., Ball, J.W., Bullen, T.D. and Sutley, S.J. (2008) Chromium, chromium isotopes and selected trace elements, western Mojave Desert, USA. Appl. Geochem. 23, 1325-1352.

Jamieson-Hanes, J.H., Gibson, B.D., Lindsay, M.B.J., Kim, Y., Ptacek, C.J. and Blowes, D.W. (2012) Chromium isotope fractionation during reduction of Cr(VI) under saturated flow conditions. Environ. Sci. Technol. 46, 6783-6789.

Jeandel, C. and Minster, J.F. (1984) Isotope dilution measurement of inorganic chromium(III) and total chromium in seawater. Mar. Chem. 14, 347-364.

Joshi, S., Wang, D., Ellis, A.S., Johnson, T.M. and Bullen, T.D. (2011) Stable Isotope Fractionation during Cr(III) oxidation by manganese oxides, American Geophysical Union, Fall Meeting 2011, abstract #EP41B-0622.

Kaczynski, S.E. and Kieber, R.J. (1994) Hydrophobic C18 bound organic complexes of chromium and their potential impact on the geochemistry of chromium in natural waters. Environ. Sci. Technol. 28, 799-804.

Karstensen, J. and Tomczak, M. (1997) Ventilation processes and water mass ages in the thermocline of the southeast Indian Ocean. Geophys. Res. Lett. 24, 2777-2780.

Kawabe, M. and Fujio, S. (2010) Pacific ocean circulation based on observation. J. Oceanogr. 66, 389-403.

Kieber, R.J. and Helz, G.R. (1992) Indirect photoreduction of aqueous chromium(VI). Environ. Sci. Technol. 26, 307-312.

Kitchen, J.W., Johnson, T.M., Bullen, T.D., Zhu, J. and Raddatz, A. (2012) Chromium isotope fractionation factors for reduction of Cr(VI) by aqueous Fe(II) and organic molecules. Geochim. Cosmochim. Acta 89, 190-201.

Klar, J.K., Homoky, W.B., Statham, P.J., Birchill, A.J., Harris, E.L., Woodward, E.M.S., Silburn, B., Cooper, M.J., James, R.H., Connelly, D.P., Chever, F., Lichtschlag, A. and Graves, C. (2017) Stability of dissolved and soluble Fe(II) in shelf sediment pore waters and release to an oxic water column. Biogeochemistry, 1-19.

Klar, J.K., Schlosser, C., Milton, J.A., Woodward, E.M.S., Lacan, F., Parkinson, I.J., Achterberg, E.P. and James, R.H. (this issue) Sources of dissolved iron to oxygen minimum zone waters on the Senegalese continental margin in the tropical North Atlantic Ocean: Insights from iron isotopes. Geochim. Cosmochim. Acta.

Li, S.-X., Zheng, F.-Y., Hong, H.-S., Deng, N.-s. and Lin, L.-X. (2009) Influence of marine phytoplankton, transition metals and sunlight on the species distribution of chromium in surface seawater. Mar. Environ. Res. 67, 199-206.

Martin, J.H., Knauer, G.A., Karl, D.M. and Broenkow, W.W. (1987) VERTEX: carbon cycling in the northeast Pacific. Deep Sea Research Part A. Oceanographic Research Papers 34, 267-285.

McClain, C.N. and Maher, K. (2016) Chromium fluxes and speciation in ultramafic catchments and global rivers. Chem. Geol. 426, 135-157.

Murray, J.W., Spell, B. and Paul, B. (1983) The Contrasting Geochemistry of Manganese and Chromium in the Eastern Tropical Pacific Ocean, in: Wong, C.S., Boyle, E., Bruland, K.W., Burton, J.D., Goldberg, E.D. (Eds.), Trace Metals in Sea Water. Springer US, Boston, MA, pp. 643-669.

Paulmier, A. and Ruiz-Pino, D. (2009) Oxygen minimum zones (OMZs) in the modern ocean. Prog. Oceanogr. 80, 113-128.

Paulukat, C., Døssing, L.N., Mondal, S.K., Voegelin, A.R. and Frei, R. (2015) Oxidative release of chromium from Archean ultramafic rocks, its transport and environmental impact – A Cr isotope perspective on the Sukinda valley ore district (Orissa, India). Appl. Geochem. 59, 125-138.

Paulukat, C., Gilleaudeau, G.J., Chernyavskiy, P. and Frei, R. (2016) The Cr-isotope signature of surface seawater — A global perspective. Chem. Geol. 444, 101-109.

Pelegrí, J.L. and Benazzouz, A. (2015) Coastal upwelling off North-West Africa, Oceanographic and biological features in the Canary Current Large Marine Ecosystem. IOC-UNESCO, Paris, pp. 93-103.

Pereira, N.S., Voegelin, A.R., Paulukat, C., Sial, A.N., Ferreira, V.P. and Frei, R. (2015) Chromium-isotope signatures in scleractinian corals from the Rocas Atoll, Tropical South Atlantic. Geobiology 14, 54-67.

Pettine, M. and Millero, F.J. (1990) Chromium speciation in seawater: The probable role of hydrogen peroxide. Limnol. Oceanogr. 35, 730-736.

Planavsky, N.J., Reinhard, C.T., Wang, X., Thomson, D., McGoldrick, P., Rainbird, R.H., Johnson, T., Fischer, W.W. and Lyons, T.W. (2014) Low Mid-Proterozoic atmospheric oxygen levels and the delayed rise of animals. Science 346, 635-638.

Rai, D., Eary, L.E. and Zachara, J.M. (1989) Environmental chemistry of chromium. Sci. Total Environ. 86, 15-23.

Reinhard, C.T., Planavsky, N.J., Robbins, L.J., Partin, C.A., Gill, B.C., Lalonde, S.V., Bekker, A., Konhauser, K.O. and Lyons, T.W. (2013) Proterozoic ocean redox and biogeochemical stasis. Proceedings of the National Academy of Sciences 110, 5357-5362.

Reinhard, C.T., Planavsky, N.J., Wang, X., Fischer, W.W., Johnson, T.M. and Lyons, T.W. (2014) The isotopic composition of authigenic chromium in anoxic marine sediments: A case study from the Cariaco Basin. Earth. Planet. Sci. Lett. 407, 9-18.

Richard, F.C. and Bourg, A.C.M. (1991) Aqueous geochemistry of chromium: A review. Water Res. 25, 807-186.

Rigaud, S., Radakovitch, O., Couture, R.-M., Deflandre, B., Cossa, D., Garnier, C. and Garnier, J.-M. (2013) Mobility and fluxes of trace elements and nutrients at the sediment–water interface of a lagoon under contrasting water column oxygenation conditions. Appl. Geochem. 31, 35-51.

Rue, E.L., Smith, G.J., Cutter, G.A. and Bruland, K.W. (1997) The response of trace element redox couples to suboxic conditions in the water column. Deep Sea Res. (I Oceanogr. Res. Pap.) 44, 113-134.

Sander, S. and Koschinsky, A. (2000) Onboard-ship redox speciation of chromium in diffuse hydrothermal fluids from the North Fiji Basin. Mar. Chem. 71, 83-102.

Saputro, S., Yoshimura, K., Matsuoka, S., Takehara, K., Narsito, Aizawa, J. and Tennichi, Y. (2014) Speciation of dissolved chromium and the mechanisms controlling its concentration in natural water. Chem. Geol. 364, 33-41.

Schauble, E., Rossman, G.R. and Taylor Jr, H.P. (2004) Theoretical estimates of equilibrium chromium-isotope fractionations. Chem. Geol. 205, 99-114.

Scheiderich, K., Amini, M., Holmden, C. and Francois, R. (2015) Global variability of chromium isotopes in seawater demonstrated by Pacific, Atlantic, and Arctic Ocean samples. Earth. Planet. Sci. Lett. 423, 87-97.

Schoenberg, R., Zink, S., Staubwasser, M. and Blanckenburg, F.v. (2008) The stable Cr isotope inventory of solid Earth reservoirs determined by double spike MC-ICP-MS. Chem. Geol. 249, 294-306.

Schroeder, D.C. and Lee, G.F. (1975) Potential transformations of chromium in natural waters. Water, Air, Soil Pollut. 4, 355-365.

Semeniuk, D.M., Maldonado, M.T. and Jaccard, S.L. (2016) Chromium uptake and adsorption in marine phytoplankton – Implications for the marine chromium cycle. Geochim. Cosmochim. Acta 184, 41-54.

Shaw, T.J., Gieskes, J.M. and Jahnke, R.A. (1990) Early diagenesis in differing depositional environments: The response of transition metals in pore water. Geochim. Cosmochim. Acta 54, 1233-1246.

Sikora, E.R., Johnson, T.M. and Bullen, T.D. (2008) Microbial mass-dependent fractionation of chromium isotopes. Geochim. Cosmochim. Acta 72, 3631-3641.

Sirinawin, W., Turner, D.R. and Westerlund, S. (2000) Chromium(VI) distributions in the Arctic and the Atlantic Oceans and a reassessment of the oceanic Cr cycle. Mar. Chem. 71, 265-282.

Stramma, L., Brandt, P., Schafstall, J., Schott, F., Fischer, J. and Körtzinger, A. (2008) Oxygen minimum zone in the North Atlantic south and east of the Cape Verde Islands. Journal of Geophysical Research: Oceans 113.

Stramma, L. and England, M. (1999) On the water masses and mean circulation of the South Atlantic Ocean. Journal of Geophysical Research 104, 20863-20883.

Stramma, L., Hüttl, S. and Schafstall, J. (2005) Water masses and currents in the upper tropical northeast Atlantic off northwest Africa. Journal of Geophysical Research: Oceans 110.

Stramma, L. and Schott, F. (1999) The mean flow field of the tropical Atlantic Ocean. Deep Sea Research Part II: Topical Studies in Oceanography 46, 279-303.

Tomczak, M. and Godfrey, J.S. (2003) Regional Oceanography: an Introduction, 2 ed. Daya Publishing House, Delhi.

Tyson, R.V. and Pearson, T.H. (1991) Modern and Ancient Continental Shelf Anoxia: An Overview. In: Tyson, R.V. and Pearson, T.H., Eds., Modern and Ancient Continental Shelf Anoxia: Geological Society of London Special Publication 58, pp. 1-24.

Wang, W.-X. and Dei, R.C.H. (2001) Influences of phosphate and silicate on Cr(VI) and Se(IV) accumulation in marine phytoplankton. Aquat. Toxicol. 52, 39-47.

Wu, W., Wang, X., Reinhard, C.T. and Planavsky, N.J. (2017) Chromium isotope systematics in the Connecticut River. Chem. Geol 224, 434-453.

Zachara, J.M., Cowan, C.E., Schmidt, R.L. and Ainsworth, C.C. (1988) Chromate Adsorption by Kaolinite. Clays Clay Miner. 36, 317-326.

Zenk, W., Klein, B. and Schroder, M. (1991) Cape Verde Frontal Zone. Deep Sea Research Part A. Oceanographic Research Papers 38, S505-S530.

Zink, S., Schoenberg, R. and Staubwasser, M. (2010) Isotopic fractionation and reaction kinetics between Cr(III) and Cr(VI) in aqueous media. Geochim. Cosmochim. Acta 74, 5729-5745.

Table 1. Terminology for the different oxygen regimes discussed in this work, after Tyson and Pearson 1991. Values converted from ml L^{-1} to µmol kg^{-1} using a seawater density value of 1.035kg L^{-1}. Note that definitions of these terms vary considerably throughout the literature.

Oxygen concentration (µmol kg^{-1})	Term used
92 - 370	Oxic
9.2 - 92	Dysoxic
0.0 – 9.2	Suboxic
0.0 (+ H$_2$S)	Anoxic

Table 2. Summary of stations sampled during this work.

Cruise	Station	Latitude	Longitude	Sea floor depth (m)	Description
D361 (*RRS* Discovery)	2	12.5942	-17.9199	2656	Slope
	3	12.6100	-17.7157	1041	Slope
	4	12.6120	-17.5728	51	Shelf
	5	12.5882	-17.5724	164	Shelf
	11.5	-2.9625	-25.6148	5300	Open ocean
	18	12.0325	-28.9805	5745	Open ocean

Table 3. Isotopic ratios for the NBS979 standard, the ^{50}Cr-^{54}Cr double spike, and mixed solutions of the sample and spike. The four stable Cr isotopes are ^{50}Cr (~4.3%), ^{52}Cr (~83.8%), ^{53}Cr (~9.5%) and ^{54}Cr (~2.4%).

	^{50}Cr/^{52}Cr	^{53}Cr/^{52}Cr	^{54}Cr/^{52}Cr
NBS979	0.05186	0.11346	0.02821
^{50}Cr-^{54}Cr double spike	19.94119	0.13753	8.72229
Target sample spike mixture	0.50740	0.11418	0.25618
Actual sample-spike mixture range (all analyses)	0.46525 - 0.57263	0.11409 - 0.11423	0.20908 - 0.25601

Table 4. Neptune MC-ICP-MS operational settings.

Collector configuration	L3	L2	L1	C	H1	H2	H3
	^{49}Ti	^{50}Cr	^{51}V	^{52}Cr	^{53}Cr	^{54}Cr	^{56}Fe
Mass resolution	5800-6500						
Integration time	4.194s						
Number of blocks	1						
Number of scans per block	100						

Table 5. Comparison of seawater $\delta^{53}Cr$ and Cr_T measurements from this study and others.

Sample	Reference	Cr_T (nmol kg^{-1})	2SD	$\delta^{53}Cr$ (‰)	2SD	n
OSIL Atlantic Salinity Standard	This work	3.10	0.04	0.97	0.10	6
	Scheiderich et al. 2015	3.02	0.06	0.96	0.06	8
Southampton Water	This work	1.31	0.06	1.48	0.06	3
	Bonnand et al. 2013	1.85	0.02	1.51	0.05	4

Table 6. Chromium data for all samples measured in this study. 2SD for $\delta^{53}Cr$ is calculated from two MC-ICP-MS measurements and reflects the analytical uncertainty (the total external reproducibility is ±0.11‰ for all samples).

Station	Depth (m)	O₂ (µmol kg⁻¹)	O₂ classification	Cr$_T$ (nmol kg⁻¹)	$\delta^{53}Cr$ (‰)	2SD	Water mass
D361 St. 2	200	70	Dysoxic	2.44	1.24	0.07	SACW
	300	58	Dysoxic	2.48	1.24	0.04	SACW
	400	44	Dysoxic	2.54	1.71	0.02	SACW
	500	50	Dysoxic	2.54	1.49	0.02	SACW
	600	57	Dysoxic	2.48	1.13	0.03	AAIW
	750	85	Dysoxic	2.67	1.18	0.05	AAIW
	900	111	Oxic	2.48	1.12	0.05	AAIW
	1700	216	Oxic	2.54	1.25	0.04	NADW
	2625	237	Oxic	2.71	1.45	0.00	NADW
D361 St.3	200	72	Dysoxic	2.50	1.28	0.07	SACW
	300	59	Dysoxic	2.54	1.30	0.01	SACW
	400	45	Dysoxic	2.54	1.23	0.01	SACW
	500	49	Dysoxic	2.62	1.15	0.05	SACW
	600	60	Dysoxic	2.56	1.24	0.02	AAIW
	700	73	Dysoxic	2.54	1.16	0.07	AAIW
	900	98	Dysoxic	2.71	1.12	0.01	AAIW
D361 St. 4	38	128	Oxic	2.13	1.28	0.00	SML
	40	112	Oxic	2.19	1.21	0.07	SML
	49	93	Oxic	2.25	1.52	0.12	SML
D361 St. 5	26	146	Oxic	2.12	1.32	0.07	SML
	36	117	Oxic	2.17	1.38	0.03	SML
	51	97	Oxic	2.21	1.40	0.09	SML
	66	82	Dysoxic	2.21	1.62	0.07	SML
	80	80	Dysoxic	2.21	1.58	0.01	SML
	107	69	Dysoxic	2.37	1.34	0.02	SML
D361 St. 18	30	210	Oxic	2.48	1.18	0.09	SML
	90	119	Oxic	2.54	1.19	0.07	SML
	225	91	Dysoxic	2.58	1.14	0.00	SACW
	400	51	Dysoxic	2.60	1.15	0.08	SACW
	600	68	Dysoxic	2.62	1.26	0.04	AAIW
	960	121	Oxic	2.69	1.09	0.04	AAIW
	2020	241	Oxic	2.54	1.13	0.04	NADW
	3550	243	Oxic	2.56	1.20	0.04	NADW
	5740	246	Oxic	2.85	1.08	0.08	NADW
D361 St. 11.5	25	202	Oxic	2.40	1.10	0.07	SML
	75	177	Oxic	2.48	1.23	0.07	SML
	100	132	Oxic	2.50	1.22	0.02	SML
	200	107	Oxic	2.54	1.20	0.02	SACW

	400	101	Oxic	2.79	1.08	0.01	SACW
	855	158	Oxic	2.90	1.21	0.02	AAIW
	1110	170	Oxic	2.71	1.72	0.05	UCDW
	1515	236	Oxic	2.50	1.20	0.09	NADW
	2020	252	Oxic	2.54	1.15	0.02	NADW

Figure 1. Locations of stations sampled in this study. Arrows show generalised direction of central (sub-surface) water mass movement (100-500m water depth) in the North Atlantic OMZ region (Stramma et al., 2008). Dashed black line is the Cape Verde Convergence Zone (Zenk et al., 1991) and red dashed line marks the approximate outline of the OMZ region.
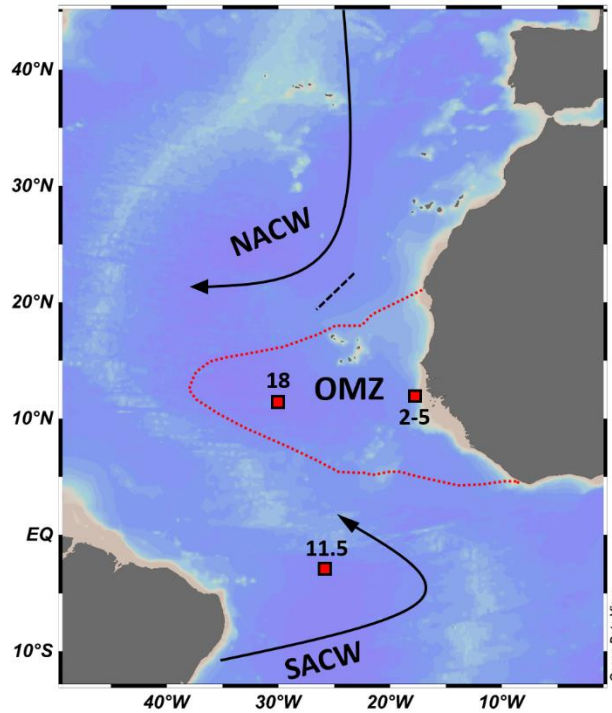
Figure 2. (A) Long term record of uncorrected NBS979 δ53Cr values made using our in-house 50Cr-54Cr double spike (n=213). (B) Long term record of NBS979 δ53Cr values made using our in-house 50Cr-54Cr double spike, normalised to the daily average NBS979 value. Area between dashed lines encompasses standards that were measured in the same analytical sessions as seawater samples reported in this study.
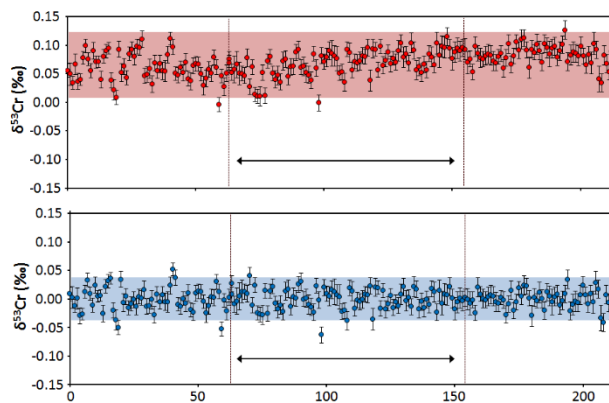
Figure 3. δ53Cr values of various seawater-standard mixtures (green circles). Seawater is from Southampton Water (SW) and the standard is NBS979. Solid black line indicates expected relationship and dashed line indicates the linear trend through measured values. Error bars are smaller than the symbols. Yellow circle shows Southampton Water doped with 10µg NBS979.
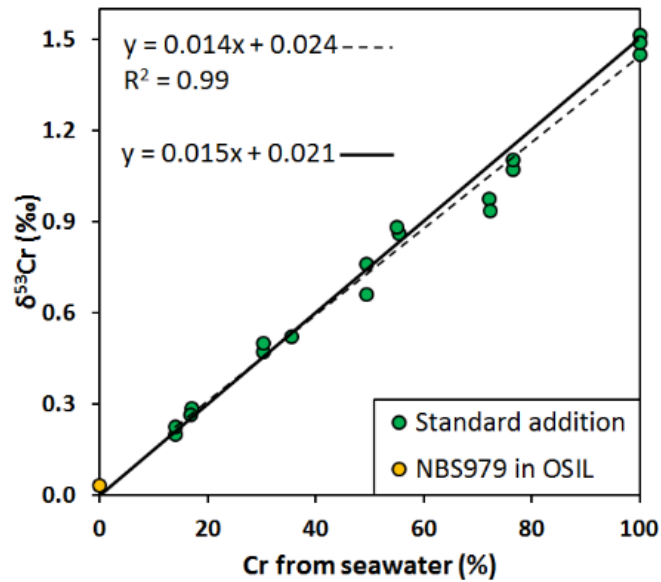
Figure 4. (A) Salinity distribution in the upper 1000m of the water column along ~12°N in the eastern tropical Atlantic showing shelf influenced North-West African waters. Black vertical lines denote stations where salinity profiles were taken. Shelf and slope stations sampled for this study (2-5) are labelled left to right. (B) Salinity profiles between 0 and 2000m water depth for all stations sampled in this study. Approximate locations of different water masses are shown by horizontal black lines. SACW = South Atlantic Central Water, AAIW = Antarctic Intermediate Water, UCDW = Upper Circumpolar Deep Water, NADW = North Atlantic Deep Water. (C) Temperature-salinity diagram for all stations (legend in B applies).
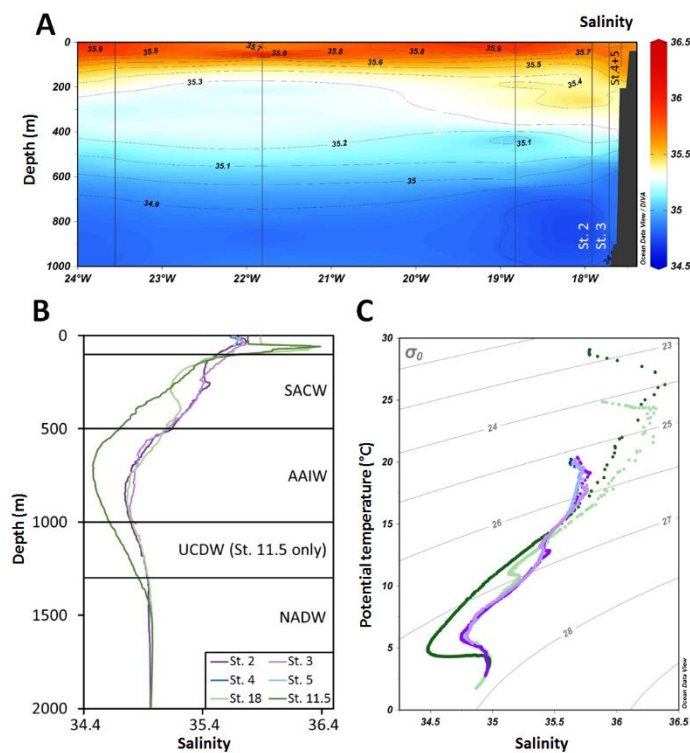
Figure 5. Profiles of O2 concentrations and Chl-a for all stations, shown in order of increasing depth.
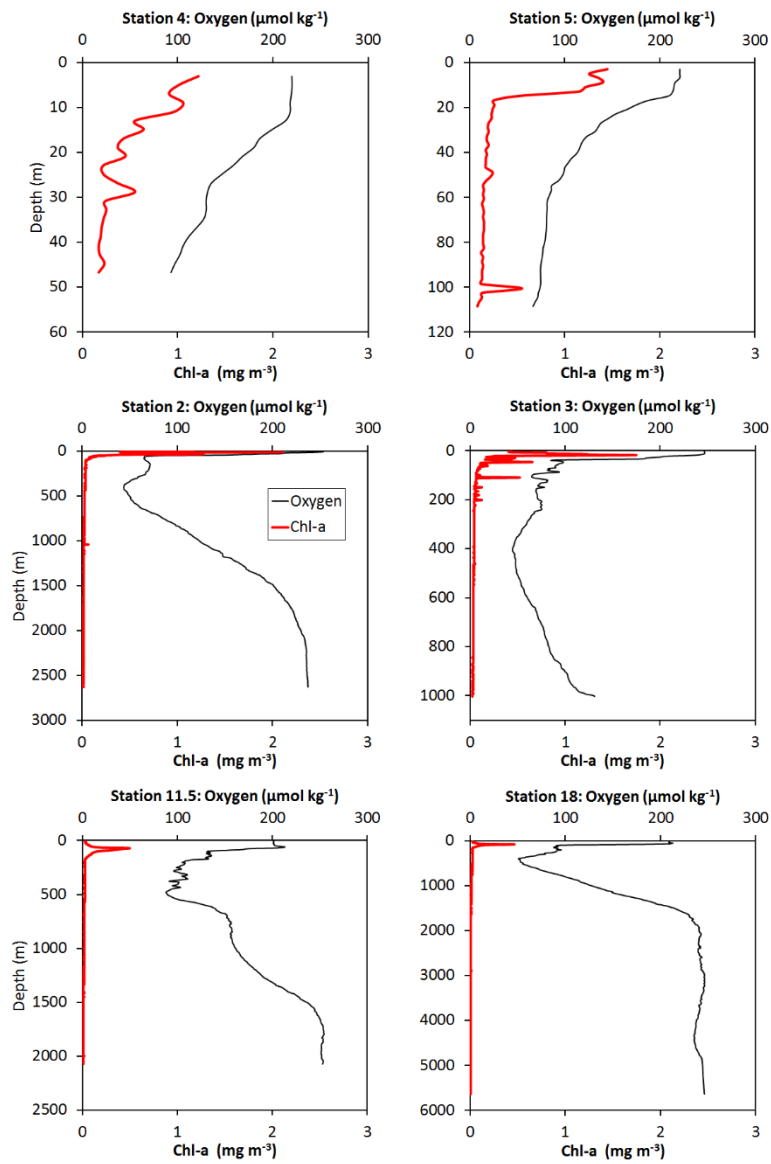
Figure 6. (A) Profiles of δ53Cr and CrT for all stations, shown in order of increasing depth.
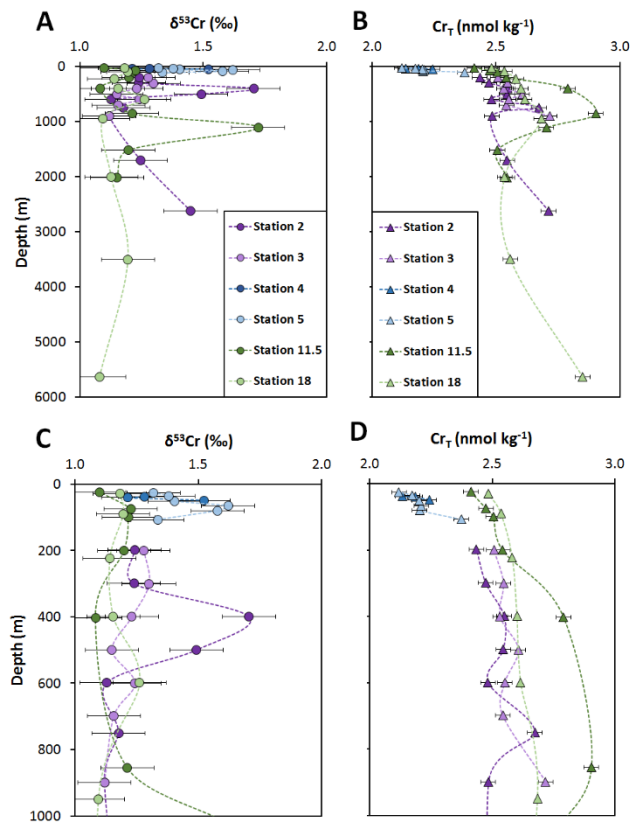(B) δ53Cr and CrT in the top 1000m water depth.

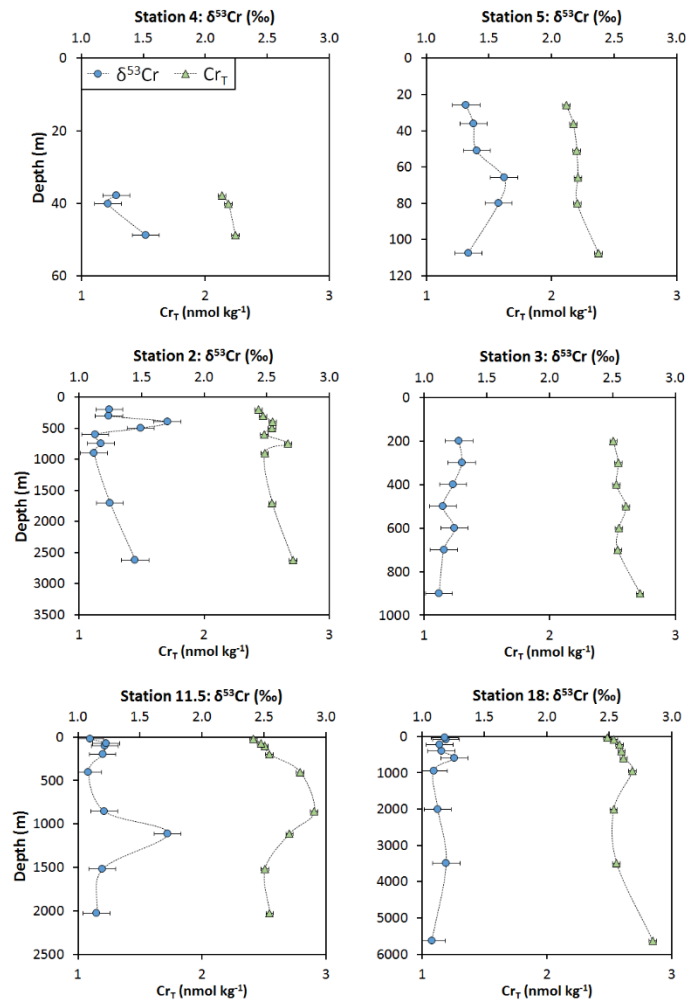Figure 7. Individual δ53Cr and CrT profiles for all stations, shown in order of increasing depth.

Figure 8. (A) CrT as a function of salinity. (B) δ53Cr as a function of dissolved O2 concentration. (C) δ53Cr as a function of light transmittance. (D) CrT as a function of O2 concentration. (E) CrT as a function of dFe concentration for shelf stations (Klar et al., this issue). (E) CrT and δ53Cr as a function of δ56Fe for shelf stations (Klar et al., this issue). Solid black lines show relationships for shelf waters (stations 4 and 5); dashed black lines show relationships for all other stations. Open circles are outliers that are excluded from trendline calculations (see text for details).
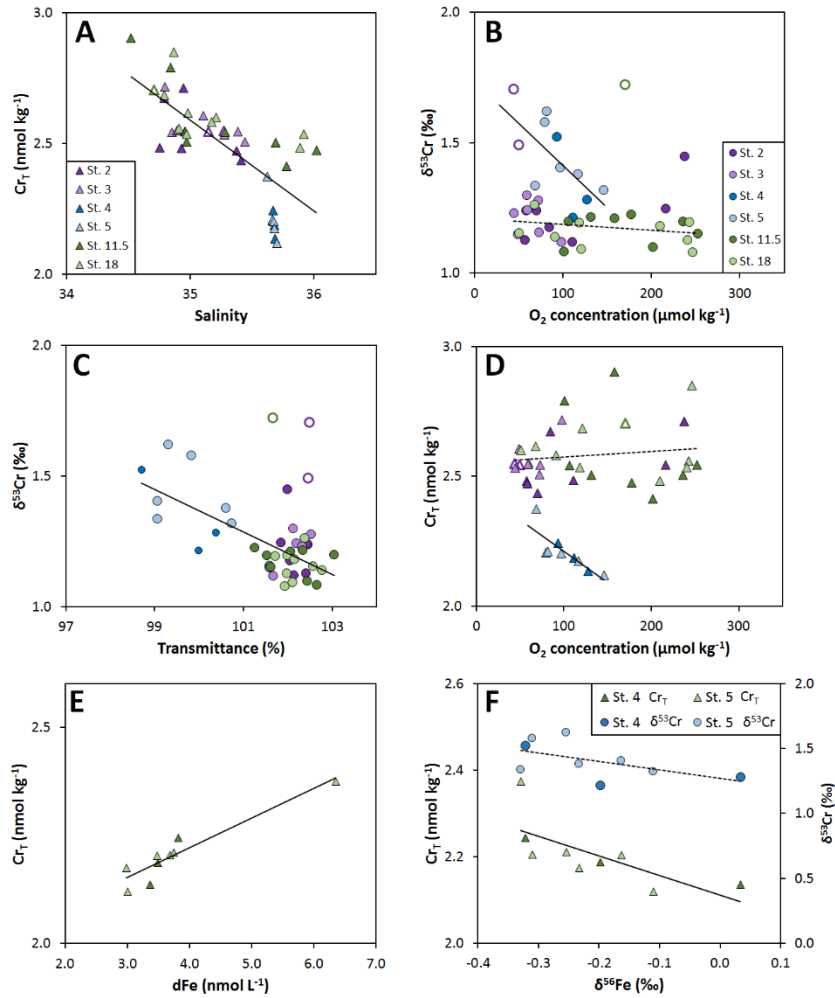
Figure 9. Correlation between δ53Cr and lnCrT for all seawater samples reported to date. Black line shows the 'global trend' line reported by Scheiderich et al. 2015. References are as follows: [1] Scheiderich et al. 2015, [2] Paulukat et al. 2016, [3] Holmden et al. 2016, [4] Paulukat et al. 2015, [5] Economou-Eliopoulos et al. 2016, [6] Bonnand et al. 2013, [7] Pereira et al. 2015.
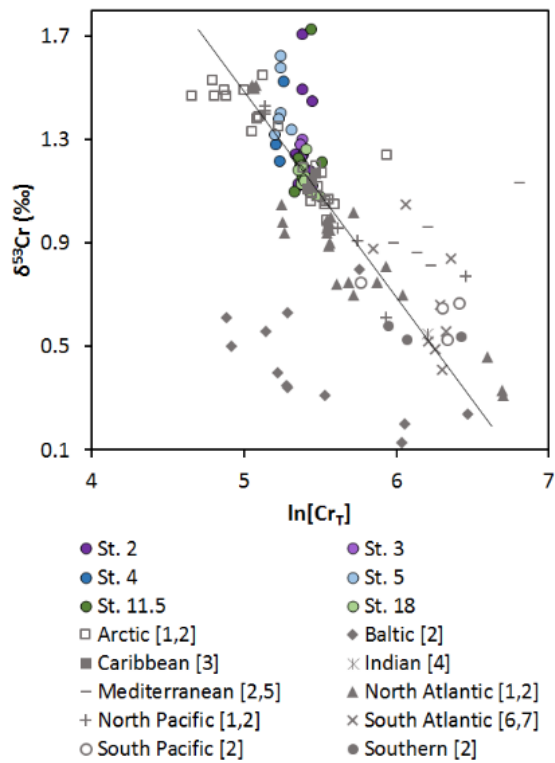

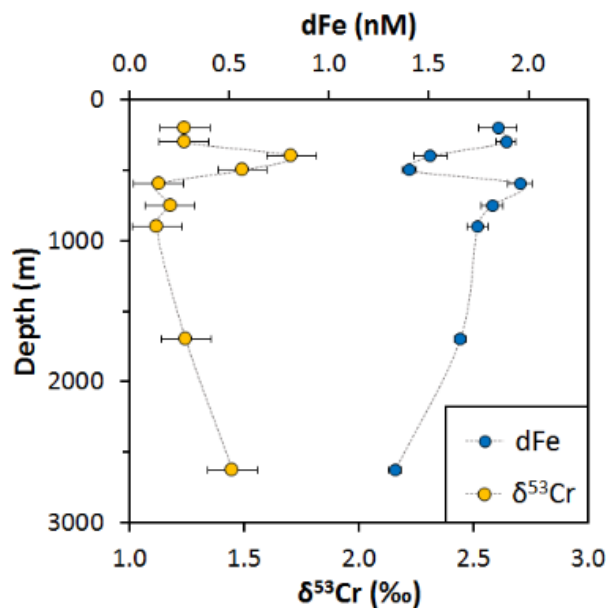Figure 10. δ53Cr and dFe profiles for Station 2 (Fe data from Klar et al., this issue).

Figure 11. Frequency plots for (A) all seawater δ53Cr data to date, except those from the Baltic Sea that may be affected by local freshwater inputs (Paulukat et al., 2016). References as for Figure 9. (B) Surface waters (<10m depth). (C) Sub-surface waters between 10-1000m depth. (D) Deep waters (>1000m depth).